

A Circuit Model for Domain Walls in Ferromagnetic Nanowires: Application to Conductance and Spin Transfer Torques

Peter E. Falloon,^{1,2,*} Rodolfo A. Jalabert,² Dietmar Weinmann,² and Robert L. Stamps¹

¹*School of Physics, The University of Western Australia, 35 Stirling Highway, Crawley WA 6009, AUSTRALIA*

²*Institut de Physique et Chimie des Matériaux de Strasbourg, UMR 7504 (CNRS-ULP), 23 rue du Loess, Boîte Postale 43, 67034 Strasbourg Cedex 2 FRANCE*

We present a circuit model to describe the electron transport through a domain wall in a ferromagnetic nanowire. The domain wall is treated as a coherent 4-terminal device with incoming and outgoing channels of spin up and down and the spin-dependent scattering in the vicinity of the wall is modelled using classical resistances. We derive the conductance of the circuit in terms of general conductance parameters for a domain wall. We then calculate these conductance parameters for the case of ballistic transport through the domain wall, and obtain a simple formula for the domain wall magnetoresistance which gives a result consistent with recent experiments. The spin transfer torque exerted on a domain wall by a spin-polarized current is calculated using the circuit model and an estimate of the speed of the resulting wall motion is made.

Introduction

Motivated by possible technological applications to non-volatile mass storage devices, the subject of spin electronics has developed into a very active area of research in recent years. Present-day state of the art devices are based on the giant magnetoresistance (GMR) effect in ferromagnetic multilayer structures, which was discovered in the late 1980's.^{1,2} Since then, several exciting developments have led to new methods of storing and switching the magnetic configuration of small magnetic elements. In particular, the use of electric currents has been proposed as an alternative method to reverse the magnetization of a magnetic layer or nanostructure.

Within this context, attention has recently turned to the use of domain walls as a possible basis for spin-electronic devices in ferromagnetic nanostructures. Studies of magnetoresistance in ferromagnetic nanowires indicate that, in addition to the well-known decrease in resistance due to the anisotropic magnetoresistance effect, there is an increase in resistance during the magnetization reversal process, which is attributed to the presence of domain walls.^{3,4} A domain wall trapped in a nanostructure can thus provide a method for storing a bit of information, as has been demonstrated in ferromagnetic nanocontacts⁵ and more recently in magnetic semiconductor nanowires.⁶ Alternatively, domain wall propagation under the influence of a spin-transfer torque induced by a spin-polarized current can be used to reverse the magnetization of a nanowire, providing a transport-based form of switching that does not require external applied fields.^{7,8,9}

Applications aside, spin transport through magnetic nanowires is also a fundamental problem in mesoscopic physics, and a growing body of theoretical work is appearing on the physics of electron transport through domain walls. In the limit of narrow walls, calculations in the ballistic regime have shown that reflection from the wall is the dominant source of resistance.^{10,11,12} This effect is large for nanocontacts, but is very small when

many transverse channels contribute, as in the case of nanowires. On the other hand, calculations valid for wide walls have shown that mistracking of electron spins traversing the wall results in an enhancement of resistance similar to the GMR effect.^{13,14} However, the latter effect has not yet been considered for domain walls of narrow or intermediate width, in which the spin mistracking becomes more significant.

In this paper we introduce a circuit model for a domain wall which combines the conductance properties intrinsic to the wall with the spin-dependent scattering occurring in the region on either side. Our model is essentially a generalization of the two-resistor model of Valet and Fert,¹⁵ which has been used to calculate the GMR effect in multilayers and interfaces. The difference is that in place of an interface, which conserves the spin of the current components, we have a domain wall, which mixes the two spin directions. We mention also that our circuit model can be considered as a specific case of a more general “magneto-electronic circuit theory” for non-homogeneous mesoscopic magnetic systems which has recently been developed.^{16,17}

The layout of this paper is as follows. In section I we introduce our circuit model and discuss the underlying physical assumptions, before deriving the resistance of the circuit in terms of the intrinsic domain wall conductance parameters in section II. In section III we derive these conductance parameters for the case of a ballistic domain wall with small spin splitting of the conduction band. We calculate the domain wall magnetoresistance within the ballistic model and compare to recent experimental results in section IV. In section V we consider the spin transfer torque exerted on the wall when a current flows and obtain a simple estimate for the resulting velocity of the wall. Finally, in section VI we discuss the limitations of our model and consider possible extensions of our work.

I. PHYSICAL DESCRIPTION OF CIRCUIT MODEL

In this section we discuss the physics underlying our circuit model. We start by assuming a simple electronic band structure, the so-called *sd* model, which consists of an *s* band of highly mobile free electrons, and a *d* band of low mobility electrons. The latter give rise to the magnetic domain structure of the ferromagnet and contribute negligibly to the conductance. The *s* electrons are subject to the effective Hamiltonian

$$H = -\frac{\hbar^2}{2m}\nabla^2 + \frac{\Delta}{2}\vec{f}(\vec{r}) \cdot \vec{\sigma}, \quad (1)$$

where $\vec{\sigma}$ is the vector of Pauli spin matrices and $\vec{f}(\vec{r})$ is a unit vector representing the direction of the local magnetization due to the *d* electrons. The back-action of the *s* electrons on the *d* electrons is neglected for the calculation of the transport properties. The energy Δ represents the strength of the spin-splitting of the *s* band induced by its interaction with the *d* band. This splitting of the up and down spin sub-bands results in a difference between the number of up and down states at the Fermi energy. Here we use “up” to refer to the majority spin sub-band of the incoming electrons, *i.e.* the one with the lower potential (and hence larger density of states at the Fermi energy E_F).

Because of the lateral confinement in the nanowire, conduction electrons occupy well-defined transverse modes. We assume for simplicity a wire with rectangular cross-section $A = L_x L_y$, so that the modes are specified by quantum numbers $n_x, n_y = 1, 2, \dots$ and energy

$$E_{\perp} = \frac{\hbar^2}{2m} \left[\left(\frac{\pi n_x}{L_x} \right)^2 + \left(\frac{\pi n_y}{L_y} \right)^2 \right]. \quad (2)$$

The number of conducting channels for the up/down spin direction, N_{\pm} , is equal to the total number of states at E_F having longitudinal energy $E_z = E_F - E_{\perp}$ in the range $-\sigma\Delta/2 \leq E_z \leq E_F$. For wires of physical interest, there is typically a large number of such states, and the number of channels is approximately $N_{\sigma} = (2mA/\pi\hbar^2)(E_F + \sigma\Delta/2)$. In this work we assume that the relative magnitude of the spin splitting is small ($\Delta \ll E_F$) so that $N_+ \simeq N_- \simeq N = 2mA E_F / \pi\hbar^2$. This assumption is valid for ferromagnetic metals, where $\Delta/E_F \simeq 0.01$ – 0.1 , but not for certain other systems, such as some magnetic semiconductors, where the polarization can be as much as 100 percent.¹⁸

In the “two-resistor” model of Valet and Fert¹⁵ the key physical assumption is that the length scale for scattering events which reverse spin direction (the so-called spin diffusion length l_{sd}) is much larger than the phase coherence length l_{ϕ} (over which the orbital part of the wavefunction loses coherence). Over length scales up to l_{sd} , the transport can thus be modelled as two resistances in parallel, representing the two spin channels.

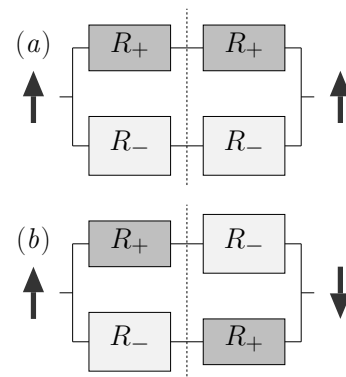


FIG. 1: The two-resistor model applied to an interface between two ferromagnetic layers, in which the magnetization is (a) parallel and (b) anti-parallel.

Since the resistivity is in general spin-dependent, this model can be used to understand the GMR of an interface between two ferromagnetic layers, *i.e.* the difference between the resistance of the parallel and anti-parallel configurations (both shown in Fig. 1). Letting R_{\pm} denote the resistance of the majority/minority spin channels over the length l_{sd} , the relative increase in resistance of the anti-parallel configuration relative to the homogeneous case is $(R_+ - R_-)^2 / 2R_+R_-$. In the anti-parallel case the currents in each channel are equal, while in the parallel case the total current has a net polarization $\beta = (R_- - R_+) / (R_+ + R_-)$.

A domain wall is a region where the magnetization direction reverses over a length which we denote 2λ (typically on the order of 10–100nm). Electronic transport through this region is characterized by a precessional motion in which the electron spins are partially reversed as they track the rotating magnetization direction.¹⁹ In the so-called *adiabatic* limit, $\lambda \rightarrow \infty$, this tracking is perfect and the spins of transmitted electrons are completely reversed upon traversing the wall. Incident majority (minority) electrons are transmitted into the majority (minority) sub-band, and hence from the point of view of resistance this limit is equivalent to a homogeneous magnetic configuration. At the other extreme is the *abrupt* limit, $\lambda \rightarrow 0$, in which electrons are transmitted with no spin reversal. In this case, incident majority (minority) electrons are transmitted into the minority (majority) sub-band, which corresponds to the antiparallel configuration of the above-mentioned two-resistor model. The physically relevant regime for domain walls in nanowires is generally intermediate between these two limits, with electrons tracking the magnetization to varying degrees depending on their longitudinal velocity.¹² The “mistracking” of the electron spin with respect to the wall magnetization results in a mixing of the up and down spin directions. Such an intermediate case is beyond the scope of the circuits in Fig. 1, and we are thus led to a modified circuit which includes the spin-mixing behaviour of the domain wall. In our circuit model the

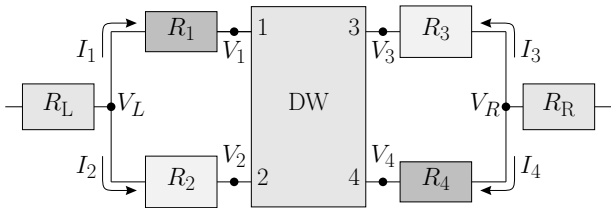


FIG. 2: The circuit model for a domain wall used in this paper.

latter is represented as a 4-terminal circuit element, connecting incoming and outgoing currents of both spin subbands.

Fig. 2 shows a sketch of our circuit model. The four-terminal element representing the domain wall (DW) is connected to resistances R_a representing the diffusive spin-dependent transport occurring over a length l_{sd} on either side of the wall. With respect to a fixed quantization axis, electrons in terminals 1 and 4 have spin $\hbar/2$, while those in terminals 2 and 3 have spin $-\hbar/2$. R_1 and R_4 are equal to the majority resistance R_+ , while R_2 and R_3 are equal to the minority resistance R_- . A key feature of the circuit is that the potentials in spin up and spin down channels close to the wall, V_1 and V_2 (V_3 and V_4), are not necessarily equal. This allows the distribution of current between the spin up and down channels to differ from that of a homogeneous wire, giving rise to a GMR-like enhancement of resistance. The spin-independent resistances R_L and R_R represent the resistance in the remainder of the wire, in which the two spin channels are equilibrated. Experimentally fabricated nanowires typically have lengths on the order of micrometers, and hence in practice $R_R, R_L \gg R_{\pm}$.

Transport in each spin channel is treated classically in the two-resistor model, since l_{ϕ} is assumed to be the smallest relevant length scale. However, domain walls can have lengths on the order of 10nm (in cobalt), or even smaller in the presence of constrictions,²⁰ which we might expect to be comparable to l_{ϕ} at liquid nitrogen temperatures. It is therefore necessary to adopt an approach based on phase coherent transport. To see how the resistances R_{\pm} arise in such an approach, we consider the incoherent transport over the length l_{sd} as a series of phase coherent segments of length l_{ϕ} . In each of these segments the transport is coherent and diffusive, with a (spin-dependent) elastic mean free path l_{\pm} and resistance $R_{\phi}^{\pm} = \frac{\hbar}{e^2} \frac{1}{N_{\pm}} \frac{l_{\phi}}{l_{\pm}}$. The total number of phase coherent segments for each spin direction is $\mathcal{N}_{\pm} = l_{sd}/l_{\phi}$, and

hence the total resistance is $R_{\pm} = \mathcal{N}_{\pm} R_{\phi}^{\pm} = \frac{\hbar}{e^2} \frac{1}{N_{\pm}} \frac{l_{sd}}{l_{\pm}}$. The spin-dependence of the resistance thus arises from differences in both N_{\pm} and l_{\pm} between the two spin subbands. In our model it is assumed that $N_+ > N_-$, but both $l_+ < l_-$ and $l_+ > l_-$ are possible. In reality, which of the latter pair of conditions is fulfilled is determined by the material-dependent band structure, which governs the number of available states at the Fermi energy into which electrons can be scattered. As mentioned previously, we assume that the difference between N_+ and N_- is rather small, and hence in our model the difference between l_+ and l_- is the dominant factor in determining the spin-dependence of the resistance.

In the remainder of this paper we use the circuit of Fig. 2 to study two main problems: domain wall magnetoresistance, in Sections II–IV, and current-driven torques, in Section V.

II. RESISTANCE OF DOMAIN WALL CIRCUIT

In this section we derive the resistance of the circuit in Fig. 2. For a general domain wall, the currents and potentials at the wall can be related by the multi-terminal Landauer-Büttiker formula:^{21,22}

$$I_a = \sum_{b \neq a} G_{ab}(V_a - V_b), \quad a, b = 1, 2, 3, 4. \quad (3)$$

The parameters G_{ab} are matrix elements of the domain wall conductance tensor for current passing between terminals a and b . Since the Hamiltonian Eq. (1) is symmetric under time-reversal (*i.e.* there is no orbital magnetic field term), these parameters satisfy $G_{ab} = G_{ba}$.²²

Eq. (3) can be written in matrix form as

$$\begin{pmatrix} I_1 \\ I_2 \\ I_3 \\ I_4 \end{pmatrix} = \begin{pmatrix} G_{11} & -G_{12} & -G_{13} & -G_{14} \\ -G_{21} & G_{22} & -G_{23} & -G_{24} \\ -G_{31} & -G_{32} & G_{33} & -G_{34} \\ -G_{41} & -G_{42} & -G_{43} & G_{44} \end{pmatrix} \begin{pmatrix} V_1 \\ V_2 \\ V_3 \\ V_4 \end{pmatrix}, \quad (4)$$

where we have defined $G_{aa} = \sum_{b \neq a} G_{ab}$. By Kirchoff's law, the terminal voltages V_a are related to the currents I_b by

$$\begin{aligned} V_1 &= V_L - I_1 R_1, & V_3 &= V_R - I_3 R_3, \\ V_2 &= V_L - I_2 R_2, & V_4 &= V_R - I_4 R_4, \end{aligned} \quad (5)$$

which allows us to rewrite Eq. (4) as

$$\begin{pmatrix} \gamma_{11} & -\gamma_{12} & -\gamma_{13} & -\gamma_{14} \\ -\gamma_{21} & \gamma_{22} & -\gamma_{23} & -\gamma_{24} \\ -\gamma_{31} & -\gamma_{32} & \gamma_{33} & -\gamma_{34} \\ -\gamma_{41} & -\gamma_{42} & -\gamma_{43} & \gamma_{44} \end{pmatrix} \begin{pmatrix} I_1 \\ I_2 \\ I_3 \\ I_4 \end{pmatrix} = \Delta V \begin{pmatrix} G_{13} + G_{14} \\ G_{23} + G_{24} \\ -(G_{13} + G_{23}) \\ -(G_{14} + G_{24}) \end{pmatrix}. \quad (6)$$

Here we have defined $\gamma_{ab} = \delta_{ab} + G_{ab}R_b$ and $\Delta V = V_L - V_R$.

Current conservation implies that $\sum I_a = 0$, which allows us to reduce the problem to a 3×3 matrix equation: changing variables to

$$x = \frac{I_1 + I_2}{2}, \quad y = \frac{I_1 - I_2}{2}, \quad z = \frac{I_3 - I_4}{2}, \quad (7)$$

we have

$$\begin{pmatrix} \gamma_{11} - \gamma_{12} + \gamma_{13} + \gamma_{14} & \gamma_{11} + \gamma_{12} & -\gamma_{13} + \gamma_{14} \\ \gamma_{22} - \gamma_{21} + \gamma_{23} + \gamma_{24} & -\gamma_{22} - \gamma_{21} & -\gamma_{23} + \gamma_{24} \\ \gamma_{33} + \gamma_{31} + \gamma_{32} - \gamma_{34} & \gamma_{31} - \gamma_{32} & -\gamma_{33} - \gamma_{34} \end{pmatrix} \begin{pmatrix} x \\ y \\ z \end{pmatrix} = \Delta V \begin{pmatrix} G_{13} + G_{14} \\ G_{23} + G_{24} \\ G_{31} + G_{32} \end{pmatrix}. \quad (8)$$

In addition to the time-reversal symmetry mentioned above, we assume a right-left symmetry with interchange of spin direction. This assumption holds for the ballistic Hamiltonian of Eq. (1), in which the potential $\vec{f}(\vec{r})$ is symmetric, but would fail if $\vec{f}(\vec{r})$ were non-symmetric or if there were an additional non-symmetric potential term (as is the case when there is disorder in the wall). Restricting ourselves to the symmetric case, the calculations simplify considerably due to the following additional equalities:

$$G_{12} = G_{43}, \quad G_{13} = G_{42}. \quad (9)$$

Since $R_1 = R_4 = R_+$ and $R_2 = R_3 = R_-$, we also have

$$\begin{aligned} \gamma_{11} &= \gamma_{44}, & \gamma_{22} &= \gamma_{33}, \\ \gamma_{12} &= \gamma_{43}, & \gamma_{21} &= \gamma_{34}, \\ \gamma_{14} &= \gamma_{41}, & \gamma_{23} &= \gamma_{32}, \\ \gamma_{13} &= \gamma_{42}, & \gamma_{31} &= \gamma_{24}. \end{aligned} \quad (10)$$

Substituting these relations into Eq. (8) and subtracting row 3 from row 2 we find $y = z$, from which it follows that $I_1 = -I_4$ and $I_2 = -I_3$. This is intuitively obvious from the symmetric structure of the circuit. We are thus left with a 2×2 system for x and y :

$$\begin{pmatrix} \gamma_{11} - \gamma_{12} + \gamma_{13} + \gamma_{14} & \gamma_{11} + \gamma_{12} - \gamma_{13} + \gamma_{14} \\ \gamma_{22} - \gamma_{21} + \gamma_{23} + \gamma_{24} & -\gamma_{22} - \gamma_{21} - \gamma_{23} + \gamma_{24} \end{pmatrix} \begin{pmatrix} x \\ y \end{pmatrix} = \Delta V \begin{pmatrix} G_{13} + G_{14} \\ G_{23} + G_{24} \end{pmatrix}. \quad (11)$$

The total resistance of the circuit between V_L and V_R is given by $R_{\text{DW}} = \Delta V / (I_1 + I_2) = \Delta V / 2x$. Solving Eq. (11) for x , we obtain

$$R_{\text{DW}} = \frac{1 + (G_{ut} + G_{uf})R_+ + (G_{dt} + G_{df})R_- + 2(G_{ut}G_{df} + G_{dt}G_{uf})R_+R_-}{G_{ut} + G_{dt} + (R_+ + R_-)(G_{ut}G_{df} + G_{dt}G_{uf})}, \quad (12)$$

where

$$\begin{aligned} G_{ut} &= G_{13} + G_{14}, & G_{dt} &= G_{23} + G_{24}, \\ G_{uf} &= G_{12} + G_{14}, & G_{df} &= G_{21} + G_{23}. \end{aligned}$$

Here G_{ut} (G_{dt}) represents the total left-to-right conductance for the incoming spin up (down) channel, while G_{uf} (G_{df}) represents the total conductance with spin flip for the incoming spin up (down) channel.

Eq. (12) is valid for arbitrary (symmetric) domain walls. The dependence on the wall structure is contained in the conductances G_{ab} . In the adiabatic and abrupt limits, these reduce to simple values and our model reproduces the expected results. In the abrupt limit there is no spin reversal and hence only G_{13} and G_{24} are non-zero. They can be calculated by summing the transmission function for each conducting channel across the interface, which has a simple closed form.¹⁵

In the adiabatic limit there is complete spin tracking, so that $G_{12} = G_{13} = G_{24} = 0$ and only G_{14} and G_{23} are non-zero. Assuming ballistic transport through the wall, we then have $G_{14} = (e^2/h)N_\uparrow$ and $G_{23} = (e^2/h)N_\downarrow$. However, for a wall in the adiabatic limit the assumption $2\lambda \lesssim l_\phi$ is unlikely to be valid, and it is more reasonable to assume diffusive transport in each spin channel. We should then take $1/G_{14} = (2\lambda/l_{sd})R_+$ and $1/G_{23} = (2\lambda/l_{sd})R_-$.

In the general case, the transport through the wall is intermediate between the adiabatic and abrupt limits and there is transmission both with and without spin reversal. In the following section, we calculate G_{ab} for the ballistic Hamiltonian of Eq. (1), which is a reasonable approximation for cobalt nanowires of the type used in Ref. 3. For wide walls (such as those in nickel for example) an approach based on diffusive transport, as used in

Refs. 13 and 14, would be more appropriate.

III. CONDUCTANCE PARAMETERS FOR BALLISTIC WALL

We now discuss the calculation of the coefficients G_{ab} for the particular case of a ballistic domain wall with small spin splitting. In this case we assume $l_{\pm} > \lambda$, so that electrons travelling through the wall experience no scattering apart from that due to the wall. We assume the magnetic structure to be one-dimensional, *i.e.* $\vec{f}(\vec{r}) \equiv \vec{f}(z)$, so that there is no scattering between different transverse modes. Micromagnetic simulations indicate that this assumption is reasonable provided the wire diameter is small enough ($L_x, L_y \lesssim 40\text{nm}$ for Co), while for wires of larger diameter more complicated structures such as vortex walls may be energetically favourable.²³

In Ref. 12 it was shown that the electron transport properties of a domain wall depend on its length and energy scales (λ and Δ) but are relatively insensitive to the precise form of the function $\vec{f}(z)$. For mathematical convenience we assume in this work a trigonometric profile

$$\vec{f}(z) = \begin{cases} (\cos(\frac{\pi z}{2\lambda}), 0, \sin(\frac{\pi z}{2\lambda})), & |z| < \lambda, \\ (0, 0, \text{sgn}(z)), & |z| \geq \lambda. \end{cases} \quad (13)$$

The spinor Schrödinger equation for the longitudinal wavefunctions with longitudinal energy $E_z = E_F - E_{\perp}$ can then be written in dimensionless form as

$$\left(\frac{d^2}{d\xi^2} + \epsilon - \begin{pmatrix} \sin(\frac{\pi\xi}{2p}) & \cos(\frac{\pi\xi}{2p}) \\ \cos(\frac{\pi\xi}{2p}) & -\sin(\frac{\pi\xi}{2p}) \end{pmatrix} \right) \Psi(\xi) = 0, \quad (14)$$

where $\epsilon = 2E_z/\Delta$, $p = \lambda\sqrt{m\Delta/\hbar^2}$ and $\xi = pz/\lambda$. The dimensionless parameter p characterizes the effective width of the domain wall, and depends on both the actual width (λ) and the spin-splitting energy (Δ). The transmission properties of a conducting state are completely determined by ϵ , the longitudinal energy measured relative to Δ .

Scattering state solutions of Eq. (14) can be found in closed form, as described in detail in the Appendix of Ref. 12. The solutions of the trigonometric wall have been used in Ref. 24, and analytic expressions to first order in $1/\lambda$ are given in Ref. 25. From these solutions we obtain transmission and reflection coefficients, $T_{\sigma\sigma'}(\epsilon)$ and $R_{\sigma\sigma'}(\epsilon)$, which give the probability for an electron incident on the left-hand side of the domain wall in the spin state σ to be transmitted or reflected into the spin state σ' . Similarly, $T'_{\sigma\sigma'}(\epsilon)$ and $R'_{\sigma\sigma'}(\epsilon)$ denote the transmission and reflection for electrons incident from the right. The conductance matrix elements G_{ab} are obtained by summing the appropriate transmission or reflection function over all states at the Fermi energy:

$$G_{ab} = \frac{e^2}{h} \sum_{n_x, n_y} F_{\sigma\sigma'}(\epsilon). \quad (15)$$

Here F denotes either T , R , T' or R' , depending on the positions of the terminals a and b ; σ and σ' denote the spin orientation in a and b .

The symmetry requirements considered above for G_{ab} also apply to the transmission coefficients: from the time-reversal symmetry of Eq. (14) we have $T_{\sigma\sigma'}(\epsilon) = T'_{\sigma'\sigma}(\epsilon)$, $R_{\uparrow\downarrow}(\epsilon) = R_{\downarrow\uparrow}(\epsilon)$ and $R'_{\uparrow\downarrow}(\epsilon) = R'_{\downarrow\uparrow}(\epsilon)$, while from the left-right symmetry of $\vec{f}(z)$ we have $R_{\uparrow\downarrow}(\epsilon) = R'_{\downarrow\uparrow}(\epsilon)$ and $T_{\uparrow\uparrow}(\epsilon) = T'_{\downarrow\downarrow}(\epsilon)$. In Ref. 12 the properties of $T_{\sigma\sigma'}(\epsilon)$ and $R_{\sigma\sigma'}(\epsilon)$ as a function of ϵ and p were studied in detail. For longitudinal energies $\epsilon > 1$, it was found that $R_{\sigma\sigma'}(\epsilon) \simeq 0$ (except for extremely narrow walls) and hence $T_{\uparrow\uparrow}(\epsilon) + T_{\downarrow\downarrow}(\epsilon) \simeq T_{\downarrow\uparrow}(\epsilon) + T_{\uparrow\downarrow}(\epsilon) \simeq 1$. Since $T_{\uparrow\uparrow}(\epsilon) = T_{\downarrow\downarrow}(\epsilon)$ by the above relations, this implies that $T_{\uparrow\downarrow}(\epsilon) \simeq T_{\downarrow\uparrow}(\epsilon)$ for $\epsilon > 1$.

In Ref. 12 the transmission and reflection functions were considered for relatively low longitudinal energies. In the present case, however, we are interested in the transmission over the full range of longitudinal energies up to ϵ_F , since this is what determines the conductances G_{ab} . In Fig. 3 we plot the functions $T_{\uparrow\uparrow}(\epsilon)$ and $T_{\uparrow\downarrow}(\epsilon)$ for several values of p with ϵ in the range 1 to 100. For all p , the transmission without spin flip ($T_{\uparrow\uparrow}(\epsilon)$) eventually goes to unity as $\epsilon \rightarrow \infty$, while the transmission with spin flip ($T_{\uparrow\downarrow}(\epsilon)$) goes to zero. Essentially, this is because states with large longitudinal energy traverse the wall rapidly and do not spend enough time in the region of rotating magnetization to undergo a complete spin reversal. As Fig. 3 shows, the energy range over which $T_{\uparrow\downarrow}(\epsilon)$ is close to unity increases with increasing p , which means that the transport through the wall becomes increasingly adiabatic as p increases. The case $p = 2.5$ shows very little spin flip, while $p = 20$ is close to the adiabatic limit and shows almost complete spin flip over the energy range considered. For intermediate values ($p = 5$), there is a co-existence of adiabatic transmission, for states with low longitudinal energy, and non-adiabatic transmission, for states with high longitudinal energy.¹² The oscillatory behaviour evident in parts (b) and (c) of Fig. 3 is a consequence of the precessional motion of the electrons in the wall.

The conductances G_{ab} are found using Eq. (15). As mentioned in Section I, we work in the case of small splitting ($\Delta \ll E_F$), which allows us to ignore those states which lie below the splitting height ($-1 < \epsilon < 1$) and consider only states with $\epsilon > 1$. As mentioned above, in this range we have $R_{\uparrow\downarrow}(\epsilon) \simeq 0$, which implies that $G_{12} \simeq 0$, and $T_{\uparrow\downarrow}(\epsilon) \simeq T_{\downarrow\uparrow}(\epsilon)$, which implies that $G_{14} \simeq G_{23}$. Furthermore, the fact that $T_{\uparrow\uparrow}(\epsilon) + T_{\uparrow\downarrow}(\epsilon) \simeq 1$ allows us to write

$$G_{13} = \frac{e^2}{h} N(1 - P), \quad G_{14} = \frac{e^2}{h} NP, \quad (16)$$

where $N \simeq 2mA E_F / \pi \hbar^2$ is the number of channels in the energy range $1 < \epsilon < \epsilon_F$ and we define

$$P = \frac{1}{\epsilon_F - 1} \int_1^{\epsilon_F} T_{\uparrow\downarrow}(\epsilon) d\epsilon. \quad (17)$$

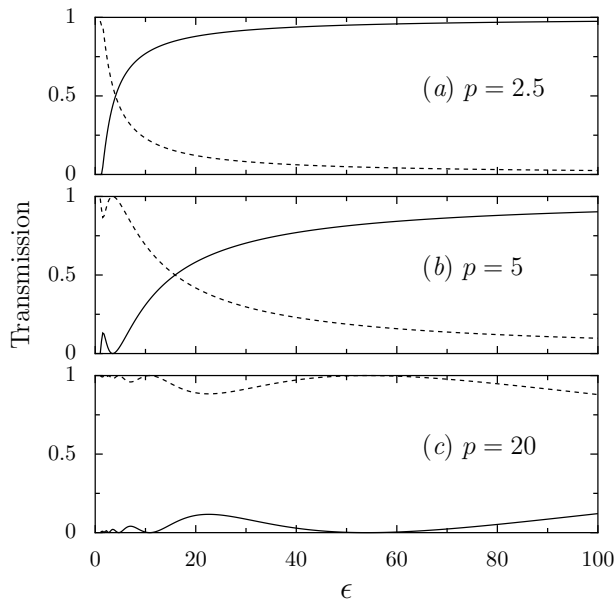


FIG. 3: Transmission functions $T_{\uparrow\uparrow}(\epsilon)$ (solid lines) and $T_{\uparrow\downarrow}(\epsilon)$ (dashed lines) as a function of ϵ ($= 2E_z/\Delta$) for p equal to (a) 2.5, (b) 5 and (c) 20.

The parameter P ($0 < P < 1$) characterizes the amount of conductance with spin flip, and is the appropriate one to describe transport since it depends not only on the characteristics of the wall (p), but also on the relation between E_F and Δ (ϵ_F). In this way, P incorporates the different degrees of adiabaticity of electrons at the Fermi energy. In Fig. 4 we show P as a function of p for $\epsilon_F = 10, 100$, calculated using Eq. (17). For all ϵ_F , there is complete spin reversal (*i.e.* $P \rightarrow 1$) in the limit $p \rightarrow \infty$. However, for smaller ϵ_F , P goes to 1 more rapidly since the adiabaticity is most pronounced for channels with small ϵ . Once again, the precessional character of the underlying electron motion through the wall gives rise to subtle oscillations in P , which are more pronounced for larger ϵ .

The approximations leading to Eq. (17) permit a considerable simplification of Eq. (12), which can now be written in the form:

$$R_{\text{DW}} = \frac{r_0(r_0 + R_+ + R_-) + (r_0(R_+ + R_-) + 4R_+R_-)P}{2(r_0 + (R_+ + R_-)P)}, \quad (18)$$

where $r_0 = h/Ne^2$ is the ballistic resistance of the nanowire. We see that the total resistance depends only on the spin-dependent resistances (R_+ and R_-), the number of channels (N) and a single parameter characterizing the adiabaticity (P).

IV. DOMAIN WALL MAGNETORESISTANCE

In our circuit model, the presence of a domain wall affects the electronic transport in a region of length

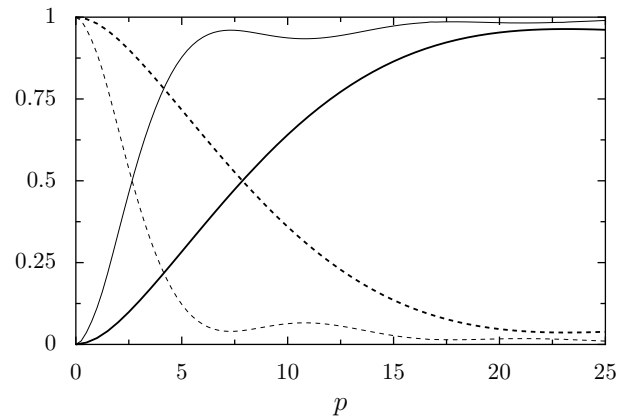


FIG. 4: Adiabaticity parameter P (solid lines) and $1 - P$ (dashed lines) as a function of the domain wall width parameter p for $\epsilon_F = 10$ (thin lines) and $\epsilon_F = 100$ (thick lines).

$2l_{sd} + 2\lambda$. Letting R_{DW} and R_0 denote the resistance of this region with and without the wall, the (relative) magnetoresistance due to the wall in a wire of total length L_{wire} and resistance R_{wire} is

$$\text{MR} = \frac{R_{\text{DW}} - R_0}{R_{\text{wire}}} = \frac{2(l_{sd} + \lambda)}{L_{\text{wire}}} \frac{R_{\text{DW}} - R_0}{R_0}. \quad (19)$$

In the case of the ballistic wall whose conductance parameters we calculated in the previous section, we can derive a particularly simple and insightful formula for the magnetoresistance. The resistance of the circuit with domain wall, R_{DW} , is given by Eq. (18). The resistance without wall, R_0 , is simply the parallel combination of spin up and down resistances, and can be formally obtained from Eq. (18) by taking the limit $P \rightarrow 1$. Substituting into Eq. (19) and assuming $r_0 \ll R_{\pm}$, we find

$$\text{MR} = \frac{l_{sd} + \lambda}{L_{\text{wire}}} \frac{2\beta^2}{1 - \beta^2} \times \frac{1 - P}{1 + \alpha P}, \quad (20)$$

where $\alpha = (R_+ + R_-)/r_0$ and $\beta = (R_- - R_+)/(R_+ + R_-)$.

Eq. (20) expresses the magnetoresistance as a product of two terms which depend on a small number of parameters. The first term corresponds to the GMR of an abrupt interface,¹⁵ and depends on the polarization β and the ratio $(l_{sd} + \lambda)/L_{\text{wire}}$. The second term, which is a function of P and α , is a “reduction factor” which decreases from 1 to 0 as P goes from 0 to 1. The behaviour of this term is shown in Fig. 5 as a function of P for several values of α . Between the abrupt ($P = 0$) and adiabatic ($P = 1$) limits, the magnetoresistance decreases monotonically from the full GMR value to zero. The rate of this transition is determined by α : near $P = 0$, where the derivative is $-(1 + \alpha)$, the rate of reduction becomes steeper with increasing α , while at $P = 1$ the derivative is equal to $-1/(1 + \alpha)$, and hence in this region the curve becomes flatter with increasing α .

Realistic values of α are reasonably large (on the order of 80 for the cobalt nanowires in Ref. 3), while the

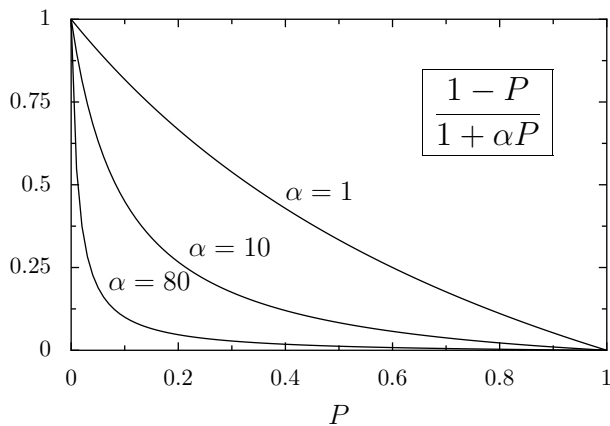


FIG. 5: The magnetoresistance, as a fraction of the GMR interface value ($P = 0$), for $\alpha = 1, 10$ and 80 .

values of P range from ~ 0.25 for cobalt to ~ 1 for nickel or permalloy. The region of Fig. 5 corresponding to realistic physical systems is thus somewhere in the “tail” region, in which the magnetoresistance is reduced by approximately an order of magnitude with respect to the GMR ($P = 0$) value. It is, however, several orders larger than the magnetoresistance predicted by a purely ballistic model, such as Ref. 12, where the resistance is completely due to reflection of conduction electrons at the domain wall.

We now compare the predictions of Eq. (20) to experiment. Ebels *et al.*³ investigated the magnetoresistance due to domain walls in cobalt nanowires of diameter 35nm and found contributions of 0.03% (based on the smallest resistance jump in Fig. 4 of Ref. 3) due to single walls in wires of length $L_{\text{wire}} \simeq 20\mu\text{m}$ and total resistance $R_{\text{wire}} = 1.4\text{k}\Omega$. Using standard material parameters for cobalt, $l_{sd} = 60\text{nm}$ and $\beta = 0.4$, the authors in Ref. 3 used the interface GMR expression (the first term on the right-hand side of Eq. (20)) to obtain a magnetoresistance of 0.14%, which is in fact larger than the experimental value. However, we must consider the reduction factor in Eq. (20) since the wall has a finite width. Assuming reasonable parameters for the band structure, $E_F = 10\text{eV}$ and $\Delta = 0.1\text{eV}$, and taking a domain wall width equal to the bulk value $\lambda = 10\text{nm}$, we find $p \simeq 5$, and our ballistic model gives $P \approx 0.25$ and $\alpha \simeq 80$. These values lead to a reduction of ~ 0.036 from the interface value and hence to a magnetoresistance of 0.0050%, which is within an order of magnitude of the experimental result of Ref. 3.

It is important to note that within a general model such as the one used in this paper, a quantitative agreement with experiment is not feasible. This is due in part to the substantial uncertainty in the parameters on which our circuit model is based: R_{\pm} , α , β and P (which depends on p and ϵ_F). Furthermore, in the case of Ref. 3, a direct comparison is complicated by the fact that the experimental results are strongly sample-dependent, and

there is some uncertainty over the number of domain walls which contribute to the magnetoresistance measured in the nanowires. Thus, an agreement to within an order of magnitude should be considered reasonable in this context.

A related issue is that in nanowires of the type fabricated in Ref. 3, domain walls tend to be pinned at local constrictions in which the wire cross-section may be significantly reduced from its average value. This leads to two effects in our model: firstly, there is an increase in r_0 , which is inversely proportional to the number of conducting channels in the wall region and hence to the cross-sectional area. Secondly, the presence of a constriction can cause a reduction in the wall width (characterized by p) from the bulk value,²⁰ resulting in a reduction in the adiabaticity, characterized by the parameter P . This is particularly important in the intermediate regime where, as Fig. 4 shows, P is rather sensitive to changes in p . As an example, consider a constriction in which the diameter and wall width are reduced by a factor of 2 in the experimental case of Ref. 3. The reduced wall width ($p \rightarrow 2.5$), gives an adiabaticity $P \simeq 0.15$ which leads, in combination with the increased r_0 , to $\text{MR} \simeq 0.03\%$, corresponding to an increase of an order of magnitude with respect to the theoretical value without constriction. The presence of a geometric constriction is thus an important factor which can significantly increase the resistance of a domain wall.

V. SPIN TRANSFER TORQUES AND DOMAIN WALL MOTION

In travelling through a domain wall conduction electrons undergo a reversal of spin in which angular momentum is exchanged with the wall. If the current incident on the wall is spin-polarized, there is an overall transfer of angular momentum from the conduction electrons to the domain wall. This gives rise to a torque on the domain wall which can cause it to move. This effect was originally predicted by Berger^{26,27} and has recently been observed in a number of experiments.^{7,8,9}

Our circuit model allows us to calculate the total torque exerted on the domain wall by summing the total spin of incoming and outgoing current components. Electrons in terminals 1 and 3 carry spin $\hbar/2$, while those in terminals 2 and 4 carry spin $-\hbar/2$. Since $I_4 = -I_1$ and $I_3 = -I_2$, there is a rate of angular momentum transfer $(\hbar/e)(I_1 - I_2)$ into the domain wall. This is equivalent to the following torque per unit current:

$$\frac{\tau}{I} = \frac{\hbar}{e} \frac{I_1 - I_2}{I_1 + I_2}. \quad (21)$$

In the abrupt (GMR) limit we have $I_1 = I_2$ and hence $\tau/I = 0$, which is expected since there is no spin reversal in this case. In the adiabatic limit, on the other hand, we have $\tau/I = \hbar\beta/e$ ($\beta = (R_- - R_+)/ (R_+ + R_-)$), which corresponds to the result obtained by Berger.²⁶ For the

intermediate case, Eq. (21) yields

$$\frac{\tau}{I} = \frac{\hbar}{e} \frac{(G_{ut} - G_{dt}) + (R_- - R_+)(G_{ut}G_{df} + G_{dt}G_{uf})}{(G_{ut} + G_{dt}) + (R_+ + R_-)(G_{ut}G_{df} + G_{dt}G_{uf})}. \quad (22)$$

For a ballistic wall, the results of the previous section yield the simple expression

$$\frac{\tau}{I} = \frac{\hbar\beta}{e} \frac{\alpha P}{1 + \alpha P}, \quad (23)$$

where α and β are as previously defined. The first part of this expression, $\hbar\beta/e$, is the adiabatic spin-transfer torque mentioned above, while the second part is a reduction factor which is less than one when there is incomplete spin reversal in the domain wall. In contrast to the magnetoresistance of the previous section, the torque becomes most significant in the adiabatic limit. We note that in our model, there is always a complete reversal of spin over the length scale of the circuit (*i.e.* $2l_{sd} + 2\lambda$); Eq. (23) gives the proportion of this which occurs in the domain wall itself.

It is important to notice that in a model considering an isolated ballistic wall (as in Ref. 12) the spin polarization of the current (and hence the resulting torque) would be proportional to Δ/E_F , and therefore very small. The inclusion of spin-dependent resistances on both sides of the wall leads to a much larger difference between up and down current components, and hence a sizeable torque.

When the precessional nature of the conduction electron motion inside the wall is taken into account it is found that, in addition to an overall component perpendicular to the local magnetization direction, there is a spatially varying torque component.²⁵ The former gives rise to motion of the domain wall, while the latter tends to induce distortions in the wall profile. However, to a first approximation it is reasonable to assume that the domain wall is “rigid” with respect to the torque exerted by the conduction electrons, so that only the total torque exerted over the domain wall length is relevant.

If the energy of the domain wall is independent of position along the wire, *i.e.* there is no pinning potential, we can obtain a simple estimate for the velocity of the wall motion which results from the spin-transfer torque. Suppose the torque τ acts on the wall for time Δt . Then in order to absorb the transferred angular momentum $\Delta S = \tau\Delta t$, the wall moves by an amount $\Delta z = \Delta S/\rho_S A$, where ρ_S denotes the angular momentum density (per unit volume) in the wire and A is the cross-sectional area. ρ_S can be determined using $\rho_S = M_S\hbar/\mu_B g$, where the saturation magnetization M_S and gyromagnetic ratio g are material-specific parameters of the ferromagnet. We thus have a simple formula for wall velocity per unit current density:

$$\frac{v_{\text{wall}}}{I/A} = \frac{1}{\rho_S} \frac{\tau}{I} = \frac{\hbar\beta}{\rho_S e} \frac{\alpha P}{1 + \alpha P}. \quad (24)$$

In a recent experiment, Yamaguchi and co-workers measured the displacement of domain walls under the

influence of current pulses of varying duration in permalloy nanowires of cross-section $240\text{nm} \times 10\text{nm}$.⁹ Assuming that the domain wall moves at constant speed, they found an average domain wall velocity of 3m s^{-1} for current pulses of density $1.2 \times 10^{12}\text{A m}^{-2}$. To compare with Eq. (24), we note that for permalloy the domain wall width is approximately $\lambda \simeq 100\text{nm}$, which gives an adiabaticity $P \simeq 1$, *i.e.* essentially completely adiabatic. Substituting typical values for the material parameters, $\beta = 0.5$, $M_S = 2\text{Tesla}/\mu_0$ and $g = 2$,²⁸ Eq. (24) gives $v_{\text{wall}} \simeq 300\text{m s}^{-1}$. This value is two orders of magnitude larger than experiment, but is in agreement with another recent calculation.²⁹ This suggests that in real physical systems the efficiency with which the spin angular momentum of the conduction electrons is transferred into motion of the domain wall is limited by other mechanisms which are not contained in the present theoretical description. In Ref. 29 it was suggested that generation of spin waves in the magnetic structure could be one such mechanism.

Finally, we note that in order for the above argument to be consistent, the constant speed of the wall, v_{wall} , should be incorporated into the Hamiltonian of the conduction electrons. The Schrödinger equation for electron states in a wire with a wall moving at constant speed can be solved in the same way as a stationary one simply by changing to the reference frame of the wall. The longitudinal wavevectors of the states will then be Doppler-reduced due to the motion of the wall. However, we have just shown that the speed of the wall is slow ($\sim 10^2\text{m s}^{-1}$ for theory, $\sim 3\text{m s}^{-1}$ for experiment) relative to the electron velocities, which for a Fermi energy of 10eV are on the order of 10^6m s^{-1} . The Doppler-reduction is therefore negligible and the conduction electron solutions for a moving wall are approximately the same as for the stationary wall.

VI. CONCLUSION

We have presented a circuit model to describe electron transport through domain walls in ferromagnetic nanowires. This model is a generalization of the GMR two-resistor model taking into account the partial reversal of spin experienced by conduction electrons traversing the wall. In the circuit, the domain wall is represented as a coherent 4-terminal device connected to classical spin-dependent resistors. The circuit model is independent of the details of the transport through the wall and is thus applicable to walls of arbitrary thickness, in which the transport can be either ballistic or diffusive.

After deriving a general formula for the resistance of the domain wall circuit, we considered the case of a ballistic wall. We identified for this case an appropriate “adiabaticity parameter” P , representing the average proportion of reversal of conduction electron spins, which characterizes completely the transport properties of the wall. Introducing some physically sound assumptions, we de-

rived a simple formula expressing the magnetoresistance of a domain wall as a product of two components: a term corresponding to the GMR of an abrupt interface and a reduction factor taking into account the partial spin reversal due to the finite width of the wall. The circuit model predicts a magnetoresistance effect which, although small relative to the interface GMR, is nevertheless much larger than that predicted by a purely ballistic model, and within an order of magnitude of the experimental results of Ref. 3.

The circuit model also allows a consideration the spin-transfer torque exerted on the domain wall due to the back-action of the conduction electrons. We obtained formulas for the torque and wall velocity per unit current, which predict a value two orders of magnitude larger than a recent experiment.⁹ This is, nevertheless, in agreement with a recent theoretical result based on an alternative approach,²⁹ suggesting that there are important physical mechanisms in these experiments which are beyond the scope of the present theoretical models.

In our model we have considered the most basic elements of the physical system in order to highlight and study the fundamental and general features of the problem. In particular, we have assumed a single spin-split parabolic band for the conduction electrons, which is the simplest non-trivial case in which to treat conduction as a problem in non-equilibrium transport. Band structure effects may indeed be significant, but most existing calculations seem to be predictive only for equilibrium properties, and there are numerous additional unsolved problems associated with nanostructures in which interfaces strongly control the underlying atomic scale structure. Calculations taking into account equilibrium band structures calculated using self consistent local density approximations³⁰ have found material-dependent changes in the resistance of up to two orders of magnitude for purely ballistic models. Allowing for the importance of band structure and screening effects, our results have nevertheless shown that the main source of resistance is

not scattering from the domain wall itself, but rather the spin-dependent scattering in the resistors on either side of the wall. We therefore expect our results to be less sensitive to the details of band structure and more strongly dependent on inelastic scattering processes.

For a more realistic treatment of the domain wall, beyond the ballistic case, it would be desirable to consider the effect of disorder in the domain wall region. The effect of electron-electron interactions also remains to be investigated. In the *sd* model, the most important interaction is between the *s* and *d* sub-bands, which we have treated using an effective field. However, this approach ignores the back-action of the *s* electrons on the *d* electrons, which could give rise to non-trivial dynamics such as spin wave excitation. We have also ignored many-body effects arising from the electron-electron interaction within the *s* band, which has recently been treated in a strictly one dimensional setting for the case of Luttinger liquids.³¹ Finally, the effect of variations in the transverse magnetic structure, such as in vortex walls, could have a significant effect on the transport properties of the domain wall, especially for wires wider than a few nanometers. In these cases additional effects on electron momentum due to the vector potential generated by the domain wall need to be taken into account, as demonstrated by Cabrera and Falicov.³²

Acknowledgments

PEF is grateful for the support of an Australian Postgraduate Award and a Jean Rogerson Fellowship from the University of Western Australia and for support from the Université Louis Pasteur in Strasbourg. This work was also supported through the Australian Research Council Linkages and Discovery Programmes and by the European Union through the RTN programme.

* Electronic address: falloon@physics.uwa.edu.au

¹ M. N. Baibich, J. M. Broto, A. Fert, F. Nguyen Van Dau, and F. Petroff, Phys. Rev. Lett. **61**, 2472 (1988).

² G. Binasch, P. Grünberg, F. Saurenbach, and W. Zinn, Phys. Rev. B **39**, 4828 (1989).

³ U. Ebels, A. Radulescu, Y. Henry, L. Piraux, and K. Ounadjela, Phys. Rev. Lett. **84**, 983 (2000).

⁴ G. Dumpich, T. P. Krome, and B. Hausmanns, J. Magn. Magn. Mater. **248**, 241 (2002).

⁵ N. García, M. Muñoz, and Y.-W. Zhao, Phys. Rev. Lett. **82**, 2923 (1999).

⁶ C. Rüster, T. Borzenko, C. Gould, G. Schmidt, L. Molenkamp, X. Liu, T. J. Wojtowicz, J. K. Furdyna, Z. G. Yu, and M. E. Flatté, Phys. Rev. Lett. **91**, 216602 (2003).

⁷ J. Grollier, D. Lacour, V. Cros, A. Hamzić, A. Vaurès, A. Fert, D. Adam, and G. Faini, J. Appl. Phys. **92**, 4825

(2002).

⁸ N. Vernier, D. A. Allwood, D. Atkinson, M. D. Cooke, and R. P. Cowburn, Europhys. Lett. **65**, 526 (2004).

⁹ A. Yamaguchi, T. Ono, S. Nasu, K. Miyake, K. Mibu, and T. Shinjo, Phys. Rev. Lett. **92**, 077205 (2004).

¹⁰ H. Imamura, N. Kobayashi, S. Takahashi, and S. Maekawa, Phys. Rev. Lett. **84**, 1003 (2000).

¹¹ D. Weinmann, R. L. Stamps, and R. A. Jalabert, in *Electronic Correlations: From Meso- to Nano-physics*, edited by T. Martin, G. Montambaux, and J. Trân Thanh Vân (EDP Sciences, Les Ulis, 2001).

¹² V. A. Gopar, D. Weinmann, R. A. Jalabert, and R. L. Stamps, Phys. Rev. B **69**, 014426 (2004).

¹³ P. M. Levy and S. Zhang, Phys. Rev. Lett. **79**, 5111 (1997).

¹⁴ E. Šimaňek, Phys. Rev. B **63**, 224412 (2001).

¹⁵ T. Valet and A. Fert, Phys. Rev. B **48**, 7099 (1993).

¹⁶ A. Brataas, Y. V. Nazarov, and G. E. W. Bauer, Phys.

- Rev. Lett. **84**, 2481 (2000).
- ¹⁷ A. Brataas, Y. V. Nazarov, and G. E. W. Bauer, Euro. Phys. J. B **22**, 99 (2001).
- ¹⁸ G. Vignale and M. E. Flatté, Phys. Rev. Lett. **89**, 098302 (2002).
- ¹⁹ M. Viret, D. Vignoles, D. Cole, J. M. D. Coey, W. Allen, D. S. Daniel, and J. F. Gregg, Phys. Rev. B **53**, 8464 (1996).
- ²⁰ P. Bruno, Phys. Rev. Lett. **83**, 2425 (1999).
- ²¹ M. Büttiker, Phys. Rev. Lett. **57**, 1761 (1986).
- ²² S. Datta, *Electron Transport in Mesoscopic Systems* (Cambridge University Press, Cambridge, 1997).
- ²³ H. Forster, T. Schrefl, D. Suess, W. Scholz, V. Tsiantos, R. Dittrich, and J. Fidler, J. Appl. Phys. **91**, 6914 (2002).
- ²⁴ A. Brataas, G. Tatara, and G. E. W. Bauer, Phys. Rev. B **60**, 3406 (1999).
- ²⁵ X. Waintal and M. Viret, Europhys. Lett. **65**, 427 (2004).
- ²⁶ L. Berger, J. Appl. Phys. **55**, 1954 (1984).
- ²⁷ L. Berger, J. Appl. Phys. **71**, 2721 (1992).
- ²⁸ R. Skomski and J. M. D. Coey, *Permanent Magnetism* (Institute of Physics Publishing, Bristol, 1999).
- ²⁹ G. Tatara and H. Kohno, Phys. Rev. Lett. **92**, 086601 (2004).
- ³⁰ J. B. A. N. van Hoof, K. M. Schep, A. Brataas, G. E. W. Bauer, and P. J. Kelly, Phys. Rev. B **59**, 138 (1999).
- ³¹ R. G. Pereira and E. Miranda, Phys. Rev. B **69**, 140402R (2004).
- ³² G. G. Cabrera and L. M. Falicov, Phys. Status Solidi B **62**, 217 (1974).